East Asian Journal on Applied Mathematics
doi: 10.4208/eajam.070217.120617a

Vol. 7, No. 3, pp. 615-628
August 2017

Simulation of a Soap Film Möbius Strip Transformation

Yongsam Kim[1], Ming-Chih Lai[2] and Yunchang Seol[3,*]

[1] *Department of Mathematics, Chung-Ang University, Dongjakgu Heukseokdong, Seoul 156-756, Korea.*
[2] *Department of Applied Mathematics, National Chiao Tung University, 1001 Ta Hsueh Road, Hsinchu 300, Taiwan.*
[3] *National Center for Theoretical Sciences, No. 1, Sec. 4, Road. Roosevelt, National Taiwan University, Taipei 10617, Taiwan.*

Received 7 February 2017; Accepted (in revised version) 12 June 2017.

Abstract. If the closed wire frame of a soap film having the shape of a Möbius strip is pulled apart and gradually deformed into a planar circle, the soap film transforms into a two-sided orientable surface. In the presence of a finite-time twist singularity, which changes the linking number of the film's Plateau border and the centreline of the wire, the topological transformation involves the collapse of the film toward the wire. In contrast to experimental studies of this process reported elsewhere, we use a numerical approach based on the immersed boundary method, which treats the soap film as a massless membrane in a Navier-Stokes fluid. In addition to known effects, we discover vibrating motions of the film arising after the topological change is completed, similar to the vibration of a circular membrane.

AMS subject classifications: 68U20, 74K35, 76D05

Key words: Möbius strip, minimal surface, twist singularity, topological change, Navier-Stokes equation, immersed boundary method.

1. Introduction

Numerical studies of a soap film Möbius strip are conducted within the fluid dynamics framework. The Möbius strip has become well known since its discovery by Möbius and Listing independently in 1858 [40]. The topological change of a minimal Möbius strip occurs when the doubly looped wire frame supporting the Möbius strip is pulled apart and gradually deformed into a planar circle.

*Corresponding author. *Email addresses:* kimy@cau.ac.kr (Y. Kim), mclai@math.nctu.edu.tw (M.-C. Lai), ycseol@ntu.edu.tw (Y. Seol)

For a smooth surface $\Sigma(t)$, the first variation of area formula is

$$\left.\frac{d}{dt}\right|_{t=0} \text{Area}\big(\Sigma(t)\big) = 2\int_{\Sigma(0)} H\,\text{dA}\,, \tag{1.1}$$

where H is the mean curvature [36]. If $H = 0$ the corresponding surface Σ can therefore have a relative minimal area, so zero mean curvature is commonly used for determination of minimal surfaces. The study of minimal surfaces with a closed boundary was initiated by Euler, and Courant investigated minimal surfaces and conducted various experiments with soap films spanning different wire frames [11]. Courant raised several questions concerning the existence and uniqueness of minimal surfaces for fixed wire frames, and the dependence of minimal surfaces on the prescribed motion of the wire frame [11].

The problem of the existence of a minimal surface with prescribed boundary conditions, known as Plateau's problem [41], has been solved independently by Douglas [13, 14] and Radó [42, 43]. Successive theoretical studies were mainly focused on more general boundary conditions, the extension of minimal surface theory in higher dimensions, and the classification of embedded minimal and periodic minimal surfaces [9,36]. In addition, numerical methods have been used to find approximate minimal surfaces — e.g. finite difference [12], finite element [4, 10, 16, 22], level set [6, 8, 35] and boundary element methods [20], and also a high-order convergent numerical scheme [47].

Although Plateau's problem has been studied in the framework of elliptic variational problems [46], for non-orientable surfaces and for surfaces with multiple junctions [21], the uniqueness of minimal surfaces and their dependence on moving boundaries have received much less attention [32, 33]. On the other hand, the continuous dependence of minimal surfaces on the prescribed motions of their boundaries is closely connected to the shapes of a soap films supported by deforming wire frames. Topological changes of the soap-films arising from the wire frame deformations have also received considerable attention, and vigorously studied using drops of viscous or inviscid fluids [17, 34], bubbles [2, 15, 24, 31], a foam structure [5, 25, 48], and a soap-film breakup [7, 18, 44]. However, the changes of minimal surfaces have been investigated for only a few simple surfaces — viz. from a catenoid to two disks when the distance between two supporting rings grows, and from a helicoid to a ribbon-shaped surface when the twist angle of two supporting helices increases [3].

The Möbius strip is a minimal surface that can be made physically. Thus by dipping an almost doubly-looped wire frame into a liquid soap, and then lifting out the wire frame and breaking the appropriate soap surfaces, the soap film remaining forms a Möbius strip — cf. Fig. 1. If the closed wire frame is gradually deformed into a planar circle, it has been found that the soap film spanning the wire can be transformed into a two-sided orientable surface. The topological change of such soap-film Möbius strips has been investigated by Goldstein *et al.* [19]. It was discovered that this process involves the collapse of the soap-film toward the wire frame and a finite-time twist singularity changing the linking number of the film's Plateau border and the centreline of the wire. The twist singularity is defined as the occurrence of a singular point on the surface accompanied by a discontinuous linking number. If the twist singularity occurs, the surface has at least a one non-regular point, and

Figure 1: Soap film Möbius strip (reproduced courtesy of R. Goldstein).

the linking number jumps from ±2 to 0 during the transformation. Based on their observations, Goldstein *et al.* [19] conjectured that the singularity associated with the topological change of the Möbius-type soap films always occurs at the wire frame.

Here we apply the immersed boundary (IB) method to study the topological transition of a one-sided non-orientable surface in a two-sided orientable surface accompanied by a finite-time twist singularity. The IB method proposed by Peskin [37] to simulate blood flow in the heart has often been used in fluid-structure interaction problems [23, 26, 27, 38, 39], and also foam dynamics where the surrounding gas is treated as a viscous incompressible fluid and the liquid foam as an immersed boundary with surface tension [28, 29]. To study the topological change of a soap-film Möbius strip, we apply the IB method from Kim *et al.* [29]. The surface of the soap film is approximated by a family of triangular facets, and the discrete force density (the surface tension) is computed at the vertices of these facets. Despite substantial differences in their edge lengths, we were able to maintain the resolution over the soap film and naturally handle the topological change of the Möbius strip. Our approach involves an interaction between the bulk fluid and the immersed materials, so it can be used in simulations rather than in theoretical studies. This means that numerically we obtain more realistic motion that distinguishes the actual physical and ideal behaviour of a given material. An interesting new phenomenon we found is a vibrating motion of the soap film similar to a circular membrane vibration, after the completion of the topological transition. The main points of the present work are:

- fluid-structure interaction modelling is used in the numerical simulation of Plateau's problem for the minimal Möbius strip;
- the appearance of a singularity due to the boundary deformation is detected; and
- a refinement of triangular meshes in the IB method is employed for our study of topological changes in the minimal Möbius strip simulation.

In Section 2, we introduce the IB method and its implementation. This method is suitable for simulation of idealised soap-film experiments to establish minimal surfaces arising during the boundary deformation. Section 3 describes the construction of the initial Möbius strip and the motion of the wire frame. The simulation results are discussed in Section 4, showing the transformation of the Möbius strip into a two-sided orientable surface accompanied by a twist singularity. We also consider the change of the throat size and the behaviour of the surface after the topological change is completed. Our final summary and conclusions are presented in Section 5.

2. Model Equations and Implementation: IB Method

In the IB method and its implementation for the simulation of a soap film spanning a closed wire immersed in a three-dimensional viscous incompressible fluid, the mass of the soap-film is ignored — i.e. we consider the soap film is a massless surface with surface tension, which allows us to incorporate the tension force into the fluid equations as a singular body force at the surface. (In passing, we note that in some cases the mass of the surface should not be ignored — e.g. in the simulation of the rupture and drainage of foams, approximate thickness parameters related to the mass of the surface have been used [45].) We consider the function $\mathbf{X}(r,s,t)$ representing the shape of a soap film at any given time t and call it the immersed boundary. Here r and s are Lagrangian coordinates. The force density $\mathbf{F}(r,s,t)$ applied to the fluid by the soap film can be computed as

$$\mathbf{F}(r,s,t) = 2\gamma H \left| \frac{\partial \mathbf{X}}{\partial r} \times \frac{\partial \mathbf{X}}{\partial s} \right| \mathbf{n}\,, \tag{2.1}$$

where γ is the surface tension constant, $\mathbf{n}$ is the unit normal vector of the surface and H denotes the mean value of two principal curvatures [29]. This formula can be derived from the variational derivative of the energy functional

$$E(\mathbf{X}) = \gamma \int \left| \frac{\partial \mathbf{X}}{\partial r} \times \frac{\partial \mathbf{X}}{\partial s} \right| dr ds\,.$$

The computation of the discrete force density is the first step to describe the shape of the soap film $\mathbf{X}(r,s,t)$ at each iteration in the simulation. However, the representation (2.1) of the force density cannot be used directly, because the soap film $\mathbf{X}(r,s,t)$ is approximated by triangular facets. Instead, we use the discrete force density defined only at the triangular vertices as the surface tension constant times the sum of areas of the triangular facets approximating the soap film [29]. In the second step, the Eulerian force density $\mathbf{f}(\mathbf{x},t)$ is derived from the Lagrangian force density $\mathbf{F}(r,s,t)$ as

$$\mathbf{f}(\mathbf{x},t) = \int \mathbf{F}(r,s,t)\delta(\mathbf{x}-\mathbf{X}(r,s,t))\,dr ds\,, \tag{2.2}$$

where $\mathbf{x} = (x,y,z)$ are fixed Cartesian coordinates and $\delta(\mathbf{x}) = \delta(x)\delta(y)\delta(z)$ is the three-dimensional Dirac delta function defining the local character of the interaction between

the force densities. We use a smoothed version of the Dirac delta function with a finite support [39], and as soon as the force density $\mathbf{f}(\mathbf{x},t)$ is determined we solve the Navier-Stokes equations for a viscous incompressible fluid

$$\rho\left(\frac{\partial \mathbf{u}}{\partial t}+\mathbf{u}\cdot\nabla\mathbf{u}\right)=-\nabla p+\mu\nabla^2\mathbf{u}+\mathbf{f}\,, \tag{2.3}$$

$$\nabla\cdot\mathbf{u}=0\,, \tag{2.4}$$

where the constants ρ and μ are the density and fluid viscosity, respectively. In order to determine the velocity field $\mathbf{u}(\mathbf{x},t)$ and the pressure $p(\mathbf{x},t)$ from these equations, we use the periodic boundary conditions and discrete Fourier transform implemented by the FFT algorithm similarly to Refs. [29,38]. After the fluid velocity field $\mathbf{u}(\mathbf{x},t)$ is determined, the nodes of the mesh located at the vertices of the triangular facets approximating the soap film moving such that

$$\frac{\partial \mathbf{X}}{\partial t}(r,s,t)=\mathbf{u}(\mathbf{X}(r,s,t),t)=\int \mathbf{u}(\mathbf{x},t)\delta(\mathbf{x}-\mathbf{X}(r,s,t)\,d\mathbf{x} \tag{2.5}$$

are updated. Eq. (2.5) is the no-slip condition corresponding to the soap film moving at the local fluid velocity. For its numerical implementation, we employ the explicit Euler method.

In summary, Eqs. (2.1)-(2.5) represent an immersed soap film interacting with a three-dimensional fluid. This system is solved numerically step by step by the above-mentioned procedure at each time level. During the computations, we have to maintain a reasonable resolution over the soap film because the nodes of the mesh move without any constraints on the edge lengths — a too coarse resolution can lead to a leak through the soap film, whereas one too fine can cause numerical instability [29]. After a time step is completed, we therefore redistribute the internal mesh nodes to maintain a suitable resolution over the surface. In particular, we check the length of each edge; and if it is larger than $h/2$ where h denotes the spatial mesh width, we add a new node halfway between the endpoints of the edge. If only one node in a triangle is added, we connect that point with the opposite vertex, thereby dividing the triangle into two new triangles. If two new nodes are added, they are connected, splitting the original triangle into a triangle and a quadrilateral, which is then split into two triangles by a diagonal. In the case where three nodes are added, we simply form new edges by connecting every pair of the new nodes. On the other hand, if the length of an edge is smaller than $h/5$ the corresponding vertices are replaced by a new one located in the middle of the corresponding edge, which removes two triangles that previously shared that edge. Any other edge that had a vertex at one of the deleted nodes is then replaced by an edge with the new vertex. However, if an edge of length smaller than $h/5$ has one end point located on the boundary of the surface, we remove the internal end point and keep the one on the wire frame. This operation also removes two triangles from the previous mesh.

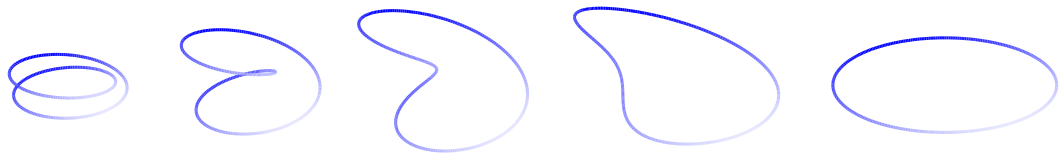

Figure 2: From left to right: the deformation of the wire frame supporting a Möbius strip for the chosen times $\tau = 0.1, 0.3, 0.5, 0.7$, and 1.0.

3. Initialisation

We construct an initial configuration for our model of a Möbius strip, and introduce physical and computational parameters used in the numerical experiments. To build a moving wire frame we use the idea of 'target boundary'. On the curve $\mathbf{X}_0(\theta,t)$ representing the wire frame, we choose target points and then apply locally the force

$$\mathbf{F}_0(\theta,t) = c_0\big(\mathbf{X}_0(\theta,t) - \mathbf{X}(\theta,t)\big) \tag{3.1}$$

to the immersed boundary points $\mathbf{X}(\theta,t)$ with a large constant c_0. The boundary points $\mathbf{X}(\theta,t)$ move at the local fluid velocity. This is a feedback mechanism for computing the boundary force needed to impose the no-slip condition. The time step is re-scaled by setting $5\tau = t$, and the motion of the target point is $\mathbf{X}_0(\theta,t) = \overline{\mathbf{X}}_0(\theta,\tau) = (x(\theta,\tau), y(\theta,\tau), z(\theta,\tau))$ where for $0 \le \theta < 2\pi$ we have

$$x(\theta,\tau) = \big(-\tau\cos\theta + (1-\tau)\cos 2\theta\big)/L(\tau), \tag{3.2}$$

$$y(\theta,\tau) = \big(-\tau\sin\theta + (1-\tau)\sin 2\theta\big)/L(\tau), \tag{3.3}$$

$$z(\theta,\tau) = 2\tau(\tau-1)\sin\theta/L(\tau), \tag{3.4}$$

and $L(\tau)$ is a scaling factor such that the length

$$l = \int_0^{2\pi} \sqrt{\left(\frac{\partial x}{\partial\theta}\right)^2 + \left(\frac{\partial y}{\partial\theta}\right)^2 + \left(\frac{\partial z}{\partial\theta}\right)^2}\, d\theta$$

of the wire frame is the same for all time steps τ in $[0.1, 1]$ — cf. Refs. [19, 30]. The initial time is set to $\tau = 0.1$, since for τ=0 the wire frame is a curve that twists a circle twice and does not allow a Möbius strip spanned along the wire frame to be built. Fig. 2 is obtained from equations (3.2)-(3.4), showing the evolution of the wire frame $\overline{\mathbf{X}}_0(\theta,\tau)$ at some chosen times. At $\tau = 0.1$, the wire frame is a two-folded circle, which becomes a large circle at τ=1 after successive deformations.

Now we build a Möbius strip spanning the wire frame at $\tau = 0.1$. The initial configuration of the Möbius strip is a developable surface with zero Gaussian curvature, made up of the line segments connecting $\overline{\mathbf{X}}_0(\theta,\tau)$ and $\overline{\mathbf{X}}_0(\theta+\pi,\tau)$, $0 \le \theta < \pi$ — cf. the left surface in Fig. 3. Since this strip is not a minimal surface, we loosen it to obtain a minimal surface – i.e. we fix the wire frame at $\tau = 0.1$ and allow the surface to evolve according to the

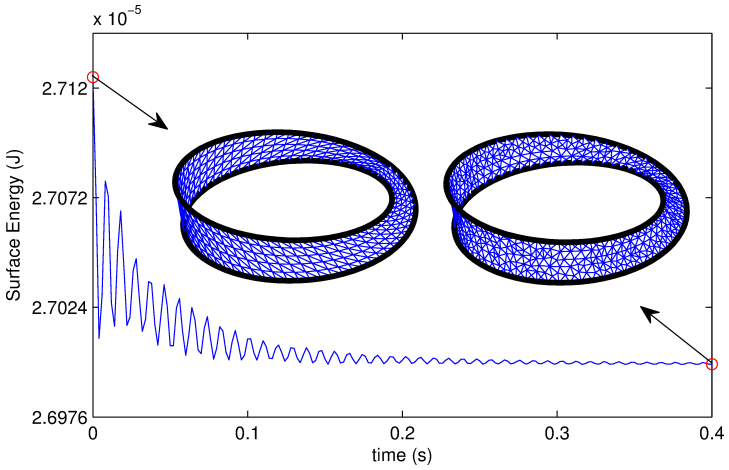

Figure 3: The initial configuration of a Möbius strip spanning the wire frame obtained from Eqs. (3.2)-(3.4) at $\tau = 0.1$. The left surface is constructed by putting together the line segments connecting $\overline{\mathbf{X}}_0(\theta,\tau)$ and $\overline{\mathbf{X}}_0(\theta+\pi,\tau)$, $0 \le \theta < \pi$ and then triangulated. The right surface approximates the minimal Möbius strip obtained by relaxation of the left surface until the total surface energy becomes almost constant, as indicated in the underlying graph.

method of the present study. Thus the initial relaxation phase of the computation proceeds until the total surface energy ($(surface\ tension\ constant) \times (total\ area)$) becomes almost constant. The right surface in Fig. 3 shows the relaxed configuration of the minimal Möbius strip, which looks more curved than the left surface. The graph in Fig. 3 shows the time-evolution of the total energy, which converges to a constant value.

The relaxed configuration of the Möbius strip has been used as a starting surface of our simulations. It was placed inside the fluid-filled cubic box $[-0.075m, 0.075m]^3$ with 64^3 grid size. The fluid density and viscosity were $\rho = 1.2\,kg/m^3$ and $\mu = 0.000018\,kg/(m\cdot s)$, respectively. They are similar to the corresponding air parameters. Typical surface tension γ of soap-films is about $0.024\,N/m$, and this value was used in our computations. The time step $\Delta t = 0.0000125s$ and the constant uniform mesh width $h = \Delta x = \Delta y = 0.15/64\,m$ were adopted, and the surface of the initial soap-film consisted of 4134 triangular facets with 2323 vertices. The typical simulation required a total of 0.5 million steps, which took about 8 hours to complete on a PC equipped with Intel i7-4770 3.4GHz CPU and 12GB memory.

4. Results and Discussions

In Ref. [19], it was observed that if a closed wire supporting a soap film Möbius strip transforms into a planar circle then the soap film changes into a two-sided orientable surface. Fig. 4 shows the motion of the surface (shaded surface) induced by the deformation of the closed wire frame (thick line) for selected times $\tau = 0.1, 0.2, 0.3, 0.415, 0.55, 0.7, 1.0$. The initial configuration of the Möbius strip is the same as the right surface in Fig. 3, and

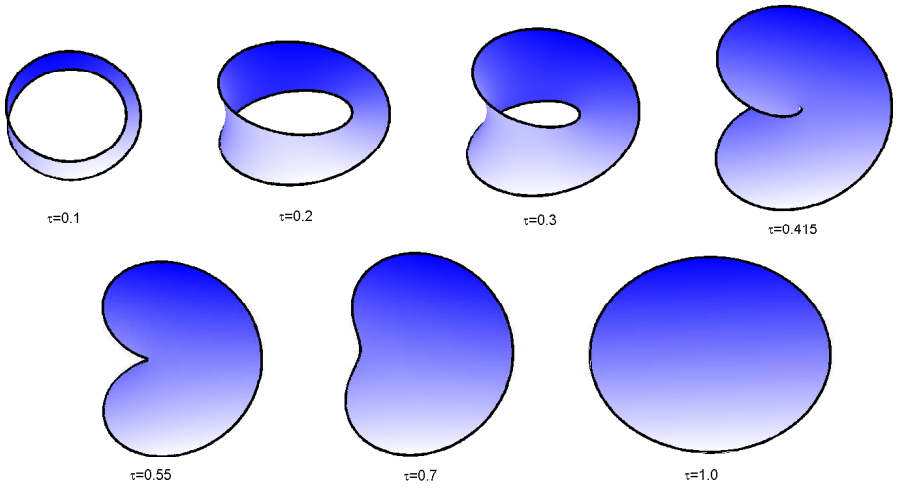

Figure 4: The surface changes induced by deformation of the closed wire frame at the times $\tau = 0.1, 0.2, 0.3, 0.415, 0.55, 0.7, 1.0$. The throat of the Möbius strip narrows and gets more concave outward, and the one-sided non-orientable surface transforms into a two-sided orientable one at about $\tau = 0.415$.

the motion of the closed wire is governed by Eqs. (3.2)-(3.4). We see that the throat of the Möbius strip gets more concave outward and its diameter diminishes. This is analogous to the catenoid that becomes more concave outward and has a smaller throat diameter as the distance between the two wire frames supporting the catenoid increases. The diameter of the throat of the Möbius strip decreases until about $\tau = 0.415$, when the Möbius strip suddenly transforms into a two-sided orientable surface shown in the second row in Fig. 4. During the transformation, the surface develops a large bent part near the throat immediately before the breakthrough and then it becomes flat, and thus we can identify an approximate time of the breakthrough by measuring the surface bending. For this, one has to compute the angle between two neighboring triangular facets approximating the surface. Fig. 5 shows the surface change together with the contours of the same angles at $\tau = 0.37, 0.415, 0.45, 0.7$ from left to right. The red and blue colours represent a large and a small bending, respectively. As one can see, the surface has a large bending part near the throat when the corresponding breakthrough happens at approximately $\tau = 0.415$. The solid line in the graph in Fig. 5 shows the maximum value of the angles over the surface as a function of time. The maximum angle increases slowly as time goes by, until approximately $\tau = 0.4$ when it rapidly jumps and achieves its maximum at $\tau = 0.415$. It then drops rapidly until $\tau = 0.45$, and then after $\tau = 0.45$ decreases slowly again. Thus it is reasonable to guess that the topological change occurs approximately at $\tau = 0.415$.

For the above calculations we adopted $t = 5\tau$ as the temporal re-scaling factor, but to see the effect of a different deformation speed of the boundary we also chose $t = 20\tau$, which leads to a slower deformation of the wire frame. Nevertheless, the change of the soap-film and the behaviour of the maximum angles are quite similar — cf. the solid and dotted lines in the graph in Fig. 5. For the case $t = 20\tau$, the sudden increase of the maximum

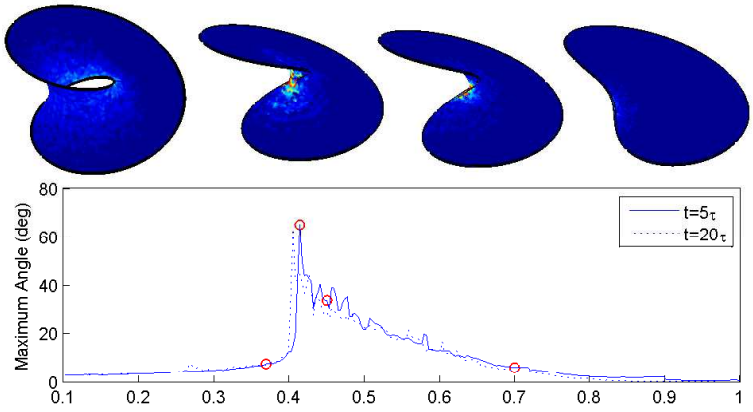

Figure 5: The surface changes at $\tau = 0.37, 0.415, 0.45, 0.7$, with red representing large bending and blue representing small bending for $t = 5\tau$. The surface has a large bending (red) near the throat when the transformation begins to occur at about $\tau = 0.415$. The underlying graph shows the maximum angle between two neighbouring triangular facets of the surface as a function of time for the cases $t = 5\tau$ (solid line) and $t = 20\tau$ (dotted line).

angle occurs at $\tau = 0.406$, slightly earlier than for $t = 5\tau$. In both cases the time of the maximum angle peak (the occurrence of a topological change) are in the overlapped range of the stable solutions for a minimal Möbius strip and a two sided orientable surface, as noted in Ref. [19].

The topological change of the Möbius strip involves the collapse of the soap film towards the wire, when there is a finite-time twist singularity changing the linking number of the film's Plateau border and the centreline of the wire [19]. Although our numerical method does not take into account the Plateau border of a finite volume, we can regard it to be the triangular facets that have one or two of their vertices on the wire frame. To find the linking number of the Plateau border and the wire frame, we construct a curve by connecting the interior vertices of the facets considered as the Plateau border. The thin blue line in Fig. 6 is the curve constructed in this way and the thick red line represents the wire frame at $\tau = 0.31, 0.415, 0.43, 0.67$. There is a visible twist between the two curves up to $\tau = 0.415$, so that the linking number is ± 2. At $\tau = 0.43$ the twist disappears and the linking number becomes 0. This confirms that the topological change of the soap film induces a twist singularity. As was seen in Fig, 4, the diameter of the throat of the Möbius strip diminishes until about $\tau = 0.415$ and finally disappears. In Fig. 7, the evolution of the Möbius strip is again seen as before. The size of the throat of the Möbius strip decreases and the cross-section of the throat in its perpendicular plane changes from a circular shape to a more elliptical one.

To see the transformation of the throat size, we calculated the diameter D of the throat, which is defined as the length of the short axis of the elliptical throat on the cross-section of the throat in the perpendicular plane — cf. the left picture in the top row of Fig. 7. The $\circ$-points in the graph in Fig. 7 show the diameter D of the throat as a function of $\tau_p - \tau$, where

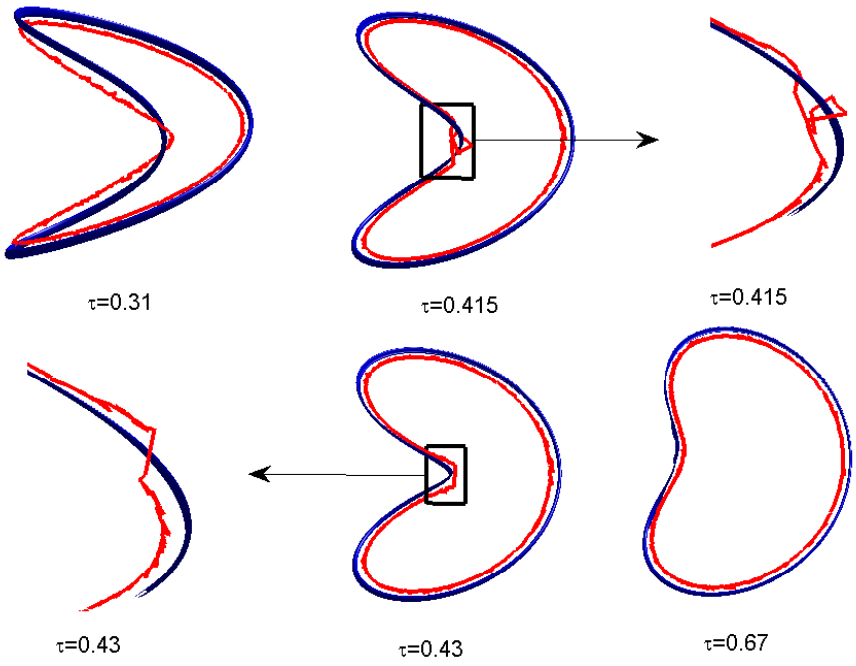

Figure 6: The wire frame (thick and blue) shown together with a curve (thin and red) constructed by connecting the vertices of the triangulated facets considered to be the Plateau border and not on the wire frame (i.e. interior points). The twist between the two curves disappears and the linking number changes from ± 2 to 0 between $\tau = 0.415$ and $\tau = 0.43$, which implies a twist singularity.

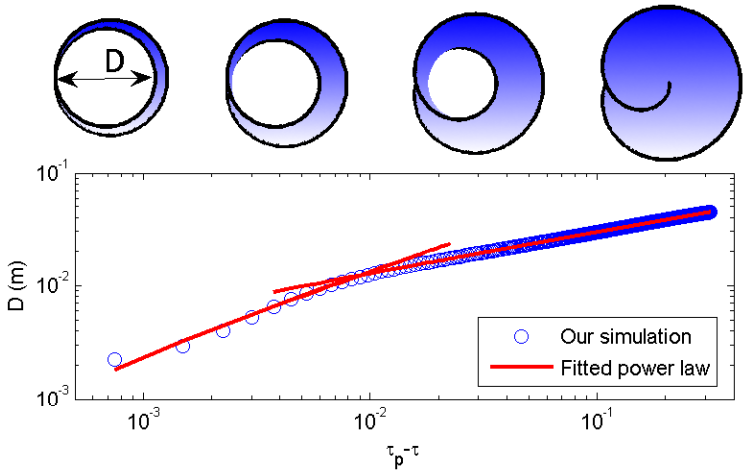

Figure 7: From left to right: view of the Möbius strip from the above perspective for $\tau = 0.1, 0.205, 0.31, 0.415$. The cross-section of the throat in its perpendicular plane transforms from a circular shape to a more elliptical one. The graph shows the diameter of the throat D as a function of $\tau_p - \tau$ where $\tau_p = 0.415$, together with the curves fitted to a least square approximation of the form $a + b(\tau_p - \tau)^c$, where a, b and c are constants.

$\tau_p = 0.415$ is an approximate collapsing time of the throat. The diameter is also fitted to a least square approximation (red curves) with a function of the form $a + b(\tau_p - \tau)^c$ where a, b and c are constants. The red curves can be divided into two parts: the left part ($\tau_p - \tau \leq 0.009$) has the power $c = 0.6762$ and the right part ($\tau_p - \tau > 0.009$) has $c = 0.3474$. Two phases in the diameter behaviour reflect the critical moment when the slow decrease of the throat diameter changes to fast, as has been also observed in experiments with comparable constants c [19].

After the deformation of the wire frame stops at $\tau = 1.0$, a remarkable vibrating motion on the soap film occurs. Fig. 8 shows the vibrating motion of the soap film and the contour representing the height of the surface with respect to the circular plane spanned by the wire frame. It is notable that the vibration of the surface is separated by the line connecting the centre of the circular plane and the point where the singularity occurs. The graph in Fig. 8 shows the height of two points on the soap film as a function of time. The ∘-line and the +-line represent the corresponding height of the ∘- point and +-point. One can see the sinusoidal oscillation of both points with a frequency of about 11 Hz, but the amplitude of the oscillation decreases in time due to the viscosity of the air.

The vibration of the soap film represented in Fig. 8 is similar to the vibration of a circular membrane modelling a timpani head [1]. In particular, it is close to the vibration of a circular membrane described by the function

$$u(r, \theta, t) = \cos(c\,\lambda\,t)\, J_1(\lambda\, r)\, \cos(\theta), \tag{4.1}$$

where r and θ are polar coordinates, u is the displacement, J_1 denotes the Bessel function of the first kind, $\lambda = 3.8371$, and c is the parameter representing the properties of the membrane. This is a standing wave which contains two crests (or troughs) in two separate regions of the circular domain. The vibration of the soap film shown in Fig. 8 also has two separate regions containing crests or troughs, but in our simulation the crest (or trough) slightly moves within each region. This particular mode of the vibration could be related to the variation of the linking number from ±2 to 0 during the topological change.

5. Summary and Conclusions

We used an immersed boundary method to study the topological change of a minimal Möbius strip induced by a prescribed motion of the boundary (wire frame). If the boundary is deformed from an almost two-folded circle into a planar circle, the soap film spanning the wire frame transforms from a one-sided non-orientable surface into a two-sided orientable surface. During the topological change of this surface, we noted effects similar to those discovered in Ref. [19] — viz. the bending in some parts of the strip increases whereas the throat of the Möbius strip diminishes and finally collapses toward the wire frame. We also found that there is a finite-time twist singularity changing the linking number of the film's Plateau border and the centreline of the wire.

After the deformation of the wire frame is completed, a vibration of the soap film occurs with two separate regions containing a moving crest or a trough. This particular mode of

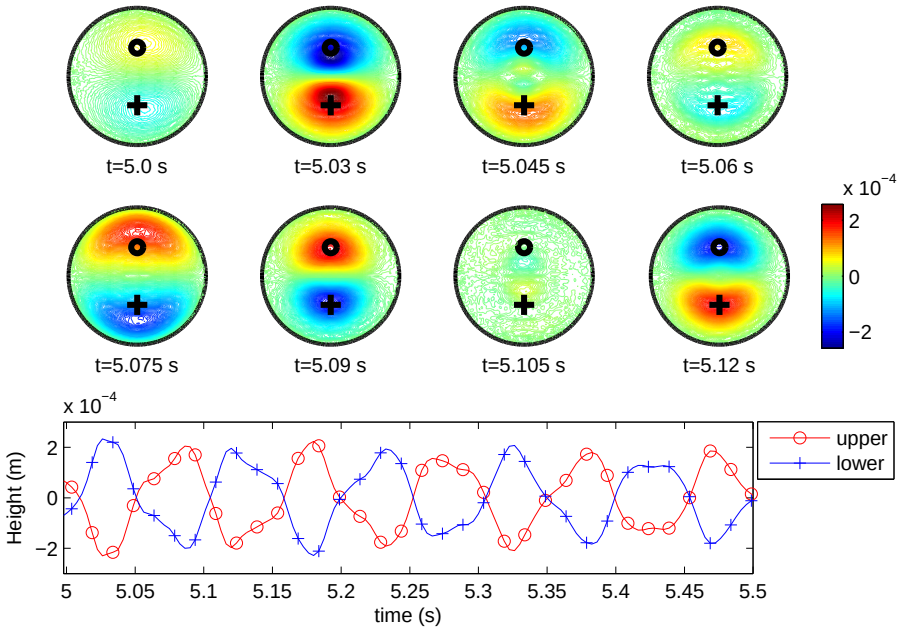

Figure 8: The motion of the vibrating surface, with contours representing the height of the surface. The graph shows the sinusoidal oscillation of the height at the two points ∘ and + on the surface as functions of time. The frequency of the oscillation is about 11 Hz, and the amplitude slowly decreases.

vibration seems to be related to the change of the linking number from ±2 to 0 during the topological change, although this requires further investigations using mathematical, computational, and experimental research tools.

Our numerical method allows us to find solution of full Navier-Stokes equations by considering the soap film as a massless surface. A general issue is how to describe the evolutionary motion of the minimal surface induced by a prescribed motion of the boundary. This can be helpful in the analysis and visualisation of deforming boundary-dependent minimal surfaces. Another open question is whether the singularity associated with the topological change of any soap film always occurs at the wire frame [19].

Acknowledgments

One of us (Y. K.) was supported by a National Research Foundation of Korea grant (Grant No. 2015R1A2A2A01005420) and by the Chung-Ang University research grant in 2015, and another (M.-C. L.) was supported in part by Ministry of Science and Technology of Taiwan under research grant MOST-104-2115-M-009-014-MY3 and NCTS.

References

[1] H. Asmar Nakhle, *Partial Differential Equations with Fourier Series and Boundary Value Problems*, Prentice Hall (2005).

[2] A.-L. Biance, S. Cohen-Addad and R. Höhler, *Topological transition dynamics in a strained bubble cluster*, Soft Matter **5**, 4672-4679 (2009).
[3] A. Boudaoud, P. Partíco and M. Amar Ben, *The helicoid versus catenoid: Geometrically induced bifurcations*, Phys. Rev. Lett. **83**, 3836-3839 (1999).
[4] K. Brakke, *The surface Evolver*, Exp. Math. **1**, 141-165 (1992).
[5] I. Cantat, S. Cohen-Addad, F. Elias, F. Graner, R. Höhler, O. Pitois, F. Rouyer and A. Saint-Jalmes, *Foams: Structure and Dynamics*, Oxford University Press (2013).
[6] T. Cecil, *A numerical method for computing minimal surfaces in arbitrary dimension*, J. Comput. Phys. **206**, 650-660 (2005).
[7] Y.-J. Chen and P.H. Steen, *Dynamics of inviscid capillary breakup: collapse and pinchoff of a film bridge*, J. Fluid. Mech. **341**, 245-267(1997).
[8] D.L. Chopp, *Computing minimal surfaces via level set curvature flow*, J. Comput. Phys. **106**, 77-91(1993).
[9] T.H. Colding and W.P. Minicozzi II, *Shapes of embedded minimal surfaces*, Proc. Nat. Acad. Sci. USA **103**, 3836-3839 (2006).
[10] P. Concus, *Numerical solution of the minimal surface equation.*, Math. Comp. **21**, 340-350 (1967).
[11] R. Courant, *Soap film experiments with minimal surfaces*, Am. Math. Mon. **47**, 167-174(1940).
[12] J. Douglas, *A method of the numerical solution of the Plateau problem*, Ann. Math. **29**, 180-188 (1928).
[13] J. Douglas, *The mapping theorem of Koebe and the problem of Plateau*, J. Math. Phys. **10** (1931) 106-130.
[14] J. Douglas, *Solution of the problem of Plateau*, Trans. Amer. Math. Soc. **33**, 263-321 (1931).
[15] M. Durand and H.A. Stone, *Relaxation time of the topological T1 process in a two-dimensional foam*, Phys. Rev. Lett. **97**, 226101 (2006).
[16] G. Dziuk and J.E. Hutchinson, *The discrete Plateau problem: Algorithm and numerics*, Math. Comp. **68**, 1-23 (1999).
[17] J. Eggers, *Nonlinear dynamics and the breakup of free-surface flows*, Rev. Mod. Phys. **69**, 865-929 (1997).
[18] A. Eri and K. Okumura, *Bursting of a thin film in a confined geometry: Rimless and constant-velocity dewetting*, Phys. Rev. E **82**, 030601(R) (2010).
[19] R.E. Goldstein, H.K. Moffatt, A.I. Pesci and R.L. Ricca, *Soap-film Möbius strip changes topology with a twist singularity*, Proc. Nat. Acad. Sci. USA **107**, 21979-21984 (2010).
[20] H. Harbrecht, *On the numerical solution of Plateau's problem*, Appl. Numer. Math. **59**, 2785-2800 (2009).
[21] J. Harrison, *Soap film solutions to Plateau's problem*, J. Geom. Anal. **24**, 271-297 (2014).
[22] M. Hinata, M. Shimasaki and T. Kiyono, *Numerical solution of Plateau's problem by a finite element method*, Math. Comp. **28**, 45-60 (1974).
[23] W.-F. Hu and M.-C. Lai, *An unconditionally energy stable immersed boundary method with application to vesicle dynamics*, East Asian J. Appl. Math. **3**, 247-262 (2013).
[24] S. Hutzler, M. Saadatfar, A. van der Net, D. Weaire, S.J. Cox, *The dynamics of a topological change in a system of soap films*, Colloid. Surface A **323**, 123-131 (2008).
[25] S.A. Jones and S.J. Cox, *The transition from three-dimensional to two-dimensional foam structures*, Eur. Phys. J. E **34**:82, (2011).
[26] Y. Kim and C.S. Peskin, *2-D parachute simulation by the immersed boundary method*, SIAM J. Sci. Comput. **28**, 2294-2312 (2006).
[27] Y. Kim and M.-C. Lai, *Simulating the dynamics of inextensible vesicles by the penalty immersed boundary method*, J. Comput. Phys. **229**, 4840-4853 (2010).

[28] Y. Kim, M.-C. Lai and C.S. Peskin, *Numerical simulations of two-dimensional foam by the immersed boundary method*, J. Comput. Phys. **229**, 5194-5207 (2010).
[29] Y. Kim, M.-C. Lai, C.S. Peskin and Y. Seol, *Numerical simulations of three-dimensional foam by the immersed boundary method*, J. Comput. Phys. **269**, 1-21 (2014).
[30] F. Maggioni and R.L. Ricca, *Writhing and coiling of closed filaments*, Proc. R. Soc. A **462**, 3151-3166 (2006).
[31] M. Le Merrer, S. Cohen-Addad and R. Höhler, *Bubble rearrangement duration in foams near the jamming point*, Phys. Rev. Lett. **108**, 188301 (2012).
[32] W.W. Meeks III and S.-T. Yau, *The existence of embedded minimal surfaces and the problem of uniqueness*, Math. Z. **179**, 151-168 (1982).
[33] J.C.C. Nitsche, *A new uniqueness theorem for minimal surfaces*, Arch. Ration. Mech. Anal. **52**, 319-329 (1973).
[34] M. Nitsche and P.H. Steen, *Numerical simulations of inviscid capillary pinchoff*, J. Comput. Phys. **200**, 299-324 (2004).
[35] S.J. Osher and J.A. Sethian, *Fronts propagating with curvature dependent speed: Algorithms based on Hamilton-Jacobi formulation*, J. Comput. Phys. **79**, 12-49 (1988).
[36] R. Osserman, *A Survey of Minimal Surfaces*, Dover Publications (2014).
[37] C.S. Peskin, *Flow patterns around heart valves: A numerical method*, J. Comput. Phys. **10**, 252-271 (1972).
[38] C.S. Peskin and D.M. McQueen, *Three dimensional computational method for flow in the heart: Immersed elastic fibers in a viscous incompressible fluid*, J. Comput. Phys. **81**, 372-405 (1989).
[39] C.S. Peskin, *The immersed boundary method*, Acta Numerica, **11**, 479-517 (2002).
[40] C.A. Pickover, *The Möbius strip: Dr. August Möbius's Marvelous Band in Mathematics, Games, Literature, Art, Technology, and Cosmology*, Basic Books (2007).
[41] J. Plateau, *Statique Expérimentale et Théoretique des Liquides Soumis aux Seules Forces Moléculaires*, Gauthier-Villars (1873).
[42] T. Rado, *The problem of the least area and the problem of Plateau*, Math. Z. **32**, 763-796 (1930).
[43] T. Rado, *On Plateau's problem*, Ann. Math. **31**, 457-469 (1930).
[44] N.D. Robinson and P.H. Steen, *Observations of singularity formation during the capillary collapse and bubble pinch-off a soap film bridge*, J. Colloid. Interf. Sci. **241**, 448-458 (2001).
[45] R.I. Saye and J.A. Sethian, *Multiscale modeling of membrane rearrangement, drainage, and rupture in evolving foams*, Science **340**, 720-724 (2013).
[46] J.E. Taylor, *Selected Works of Frederick J. Almgren, Jr.*, American Mathematical Society (1999).
[47] Ø. Tråsdahl and E.M. Rønquist, *High order numerical approximation of minimal surfaces*, J. Comput. Phys. **230**, 4795-4810 (2011).
[48] D. Weaire and S. Hutzler, *The Physics of Foams*, Oxford University Press (1999).